Fibrous composite material for textile heart valve design: *In vitro* assessment

Simon Amna Amri[1,3], Nabil Chafke[2], Frederic Heim[1], and Gaétan Laroche[3,4]

[1]*Laboratoire de Physique et Mécanique Textiles EA 4365, ENSISA, Geprovas, Mulhouse, France*
[2]*Service de Chirurgie Vasculaire-Geprovas, Hôpitaux Universitaires de Strasbourg, Strasbourg, France*
[3]*Québec Biomaterials Institute, Hôpital St-François d'Assise, CHUQ, 10 rue de l'Espinay, Québec, Québec, Canada*
[4]*Department of Surgery, Faculty of Medicine, Laval University, Quebec, Québec, Canada*

ABSTRACT
With over 150.000 implantations performed over the world, transcatheter aortic valve replacement (TAVR) has become a surgical technique, which largely competes open surgery valve replacement for an increasing number of patients. The success of the procedure favors the research towards synthetic valve leaflet materials as an alternative to biological tissues, which durability remains unknown. In particular, fibrous constructions have recently proven durability in vivo over a 6 months period of time in animal sheep models. Exaggerated fibrotic tissue formation remains, however, a critical issue to be addressed. This work investigates the design of a composite fibrous construction combining a woven PET layer and a non-woven PET mat, which are expected to provide respectively strength and appropriate topography towards limited fibrotic tissue ingrowth. For that purpose, a specific equipment has been developed to produce slight non-woven PET mats. These mats were assembled with woven PET substrates using various assembling techniques in order to obtain hybrid fibrous constructions. The physical and mechanical properties of the obtained materials were assessed, and valve samples were manufactured to be tested in vitro for hydrodynamic performances. Results bring out that the composite fibrous construction is characterized by properties suitable for the valve leaflet function, but the durability of the assembling is however limited under accelerated cyclic loading.

KEYWORDS
Fibrous composite, heart valve, TAVR, textile composite, textile valve, transcatheter valve, valve fibrosis.

CITATION
Amri, A., Laroche, G., Chakfe, N., & Heim, F. (2018). Fibrous composite material for textile heart valve design: in vitro assessment. Biomedical Engineering/Biomedizinische Technik, 63(3), 221-230.

1 INTRODUCTION

Over the last decade, transcatheter aortic valve replacement (TAVR) has become an accepted alternative technique to surgical valve replacement for over 150 000 patients worldwide[1,2,3,4]. This non-invasive technique provides increased comfort to the patient, but is today mainly used for critical patients who cannot undergo classic surgery. However, in a fast-growing global market, where

TAVR related survival rates depend highly on the initial patient's health, one can expect that less-critical patients could be treated successfully with TAVR in the coming years.

Currently, the valve material used in the TAVR procedure is biologic tissue, such as bovine or porcine pericardium. This material has been extensively used in open heart valve surgery over the last decades and remains the gold standard. However, there is lack of data about the long-term durability of biological tissue used in trans-catheter devices. A few studies about TAVR have shown that, once assembled inside the metallic stent and crimped at low diameter for catheter insertion, the biological material undergoes additional stress and gets already degraded before implantation[5,6,7]. A first long term durability study about first generation devices has been recently presented and shows high rates of valve degeneration after a few years[8]. In addition, devices made from biological leaflets remain expensive due in particular to the harvesting costs of biological tissue. At last, future devices should be manufactured at lower diameter in order to be inserted more easily through generally already diseased artery networks. For that purpose, there's a need for leaflet material, which could be less thick than existing materials.

In this context, it is of interest to investigate the potential of synthetic leaflet material alternatives and fibrous constructions could be considered as interesting candidates to replace the biological tissue leaflets in the TAVR procedures. Textile material is characterized by outstanding flexibility and strength and can be manufactured with very low thickness at low cost. It can be easily folded to low diameter for catheter insertion purpose. With respect to material durability it has been proven that woven textile considered as valve leaflet material could sustain largely over 200 Mio loading cycles[9]. Moreover, regarding interaction with biological tissue, synthetic fibrous material should be at least as performant as biological tissue. In particular, fibrotic tissue ingrowth should be limited in order to keep the leaflet material flexible. But one of the limits of textile materials is their roughness due to the yarn crossing and surface discontinuity. Basically, the standard foreign body reaction (FBR), which is characterized by the encapsulation of the synthetic leaflets in fibrotic tissue, is largely influenced by the topography of the leaflet surface. Being porous, textile material may be specifically prone to fibrotic tissue ingrowth. This behavior may depend on the size and number of the pores as well as on the topography of the yarns that are involved in the textile construction[10,11,12,13]. Actually, with a thick fibrotic tissue layer growing in the fabric, the movement of the leaflet would be limited, and this must be avoided.

Preliminary in vivo implantations of textile valves have been performed recently in sheep models over a 6 months period of time and reported in literature14. Results bring out that the interaction between the porous fibrous surface and the biological tissue leads to fibrosis formation. By comparing various textile constructions, it has, however, been shown that the phenomenon depends on the size of the filaments and the size of the pores. In particular, materials fabricated from multifilament yarns with 10 µm filament diameter are characterized by limited fibrosis development when compared to monofilament yarn materials with larger diameter, e.g. 30 µm. This is in agreement with other results from the literature[15,16,17,18]. Actually, the formation of fibrotic tissue is limited on substrates characterized by larger pores and reduced fiber size. Fibroblasts spread preferentially in a 2D pattern and avoid wrapping around fibers characterized by curvature radii lower than 10-15 µm and larger than 3-5 µm[15,16]. Moreover, large distance between fibers prevent fibroblasts from bridging between 2 neighbor fibers. Actually, considering all these aspects, non-woven material made from distant low diameter fibers would present an advantage regarding the interaction with fibroblasts. Over the last years, several research projects have already focused on investigating the potential of non-woven fibrous scaffolds for valve tissue engineering[19,20,21] but with no convincing results regarding the long term durability as the material is characterized by limited strength due to the lack of cohesion in the fibrous structure. In this context, the approach consisting in combining a woven construction with a non-woven mat in a hybrid textile construction deserves investigation. This hybrid construction is likely to combine the strength of the woven textile with the appropriate surface roughness, provided by the non-woven mat. This combination is expected to provide more durable valve leaflets.

The purpose of this work was to design a specific fibrous construct combining a woven PET layer and a non-woven PET mat, providing mechanical strength and appropriate topography to the construction. A force spinning device was set up in order to produce PET non-woven layers made from low diameter fibers. The non-woven mats were then assembled with woven constructions considering different assembling methods. The obtained hybrid textile membrane was characterized for physical and mechanical properties and shaped into valves. Finally, the durability of the obtained hybrid valves was assessed.

2 MATERIALS AND METHODS

2.1 Non-woven PET production

Non-woven PET fibers mats were obtained with a force spinning system. This technology was preferred to electrospinning, which is classically used to produce low diameter non-woven fibrous mats (nanoscale). Actually, electrospun nanofiber mats, in which fibers are very close together, tend to promote fibroblasts bridging, which is to be avoided for the valve application. Moreover, the process requires the use of PET solvents, which are delicate to manipulate and in this first approach, focusing on PET material was a priority as the material is considered as largely biocompatible. The force spinning method allows producing enough distanced fine PET fibers from melted PET polymer using the centrifugal force effect. For that purpose, a dedicated system has been developed in house composed of a motor, an infrared heater, a rotary reservoir equipped with a nozzle. The polymer is heated up to melting temperature (260°C). When the reservoir rotates, the centrifugal force induces a jet of the melted polymer through the nozzle. Due to the temperature gradient, the jet is solidified and non-woven fibers are formed (Figure1).

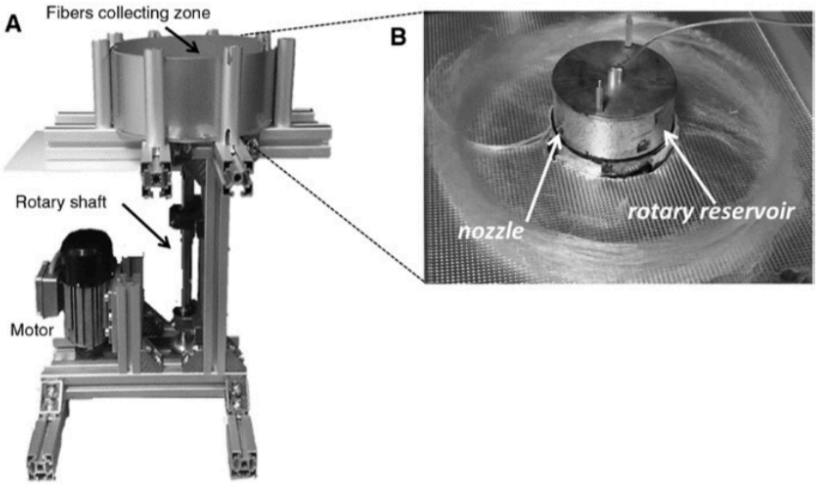

Figure 1. (A) Force Spinning system (B) Upper part of the Force Spinning system: the collector with the rotary reservoir.

2.2 Influence of the materials parameters on the non-woven properties (fiber size and distribution)

The non-woven layer properties, in particular the diameter of the fibers and their distribution, were tunable by varying the nozzle diameter, the angular velocity of the reservoir and the viscosity. The effect of those parameters was investigated in order to choose the appropriate operating conditions that enabled the production of fibers around 10 µm.

Actually, the force spinning process involves two competing forces, which control both the fiber average diameter size and the fiber diameter distribution. On one hand, a higher centrifugal force,

which is directly related to the angular velocity, enhances the stretching of the fibers, therefore leading to a decrease of their average diameter. On the other hand, the viscous force, related to the polymer temperature, tends to restrain the stretching of the fibers. Moreover, the throughput of polymer, which depends on the nozzle diameter, will influence the size of the fiber as well. In order to reduce the size of the fibers, all these parameters were considered.

With respect to the nozzle, a commercially available 0.2 mm diameter nozzle was chosen, and non-woven mats with large fibers (35 μm, sample A) could be easily obtained in a first approach at low angular velocity (4700 rpm). However, with that nozzle, angular velocity had to be set at 6000 rpm in order to produce low diameter fibers, and the viscosity had to be set accordingly. Actually, viscosity of the melted polymer could be tuned through varying the heating temperature according to the Arrhenius-Eyring equation:

$$\eta = A \cdot exp\left(\frac{E}{RT}\right) \quad (1)$$

Where (η) is the viscosity at temperature (T), (R) is the gas constant, (A) is the frequency term depending on the entropy of activation for flow and (E) is the activation energy for viscous flow (E = 20 Kcal/mol for PET). In the frame of this work only a relative viscosity value has been calculated without considering the proportional coefficient (A) for comparison purpose. Finally, at 6000 rpm, by decreasing the relative viscosity from 0.98 (260°C) to 0.96 (270°C) it was possible to decrease the average diameter of the fibers from 11μm (sample B) down to 4 μm (sample C) (Table 1). In all cases fibers appear to be uniform and continuously stretched without breaking. Figure 2 shows typical fiber distribution for the various obtained mats (sample A, sample B and sample C). All mats look cohesive, but however fragile when fiber size is too low (sample C). When a larger relative viscosity value is considered (temperature lower than 250°C) it becomes difficult to expel the polymer jet out of the nozzle because the centrifugal force fails to overcome the viscous force. The obtained fiber becomes irregular.

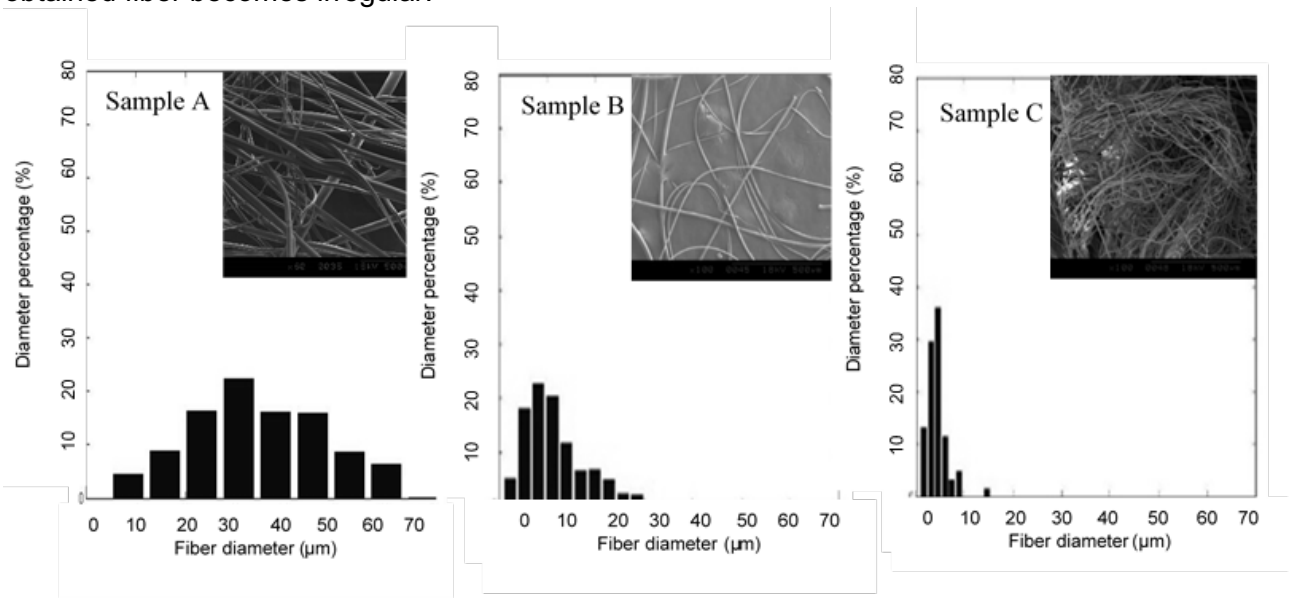

Figure 2. Scanning electron micrographs of fibers spun at different viscosities, their diameter distribution and their characteristics.

Table 1. Average fiber diameter for non-woven mats spun at different viscosities

	Sample A	Sample B	Sample C
Angular velocity (rpm)	*4700*	*6000*	*6000*
Viscosity	*1*	*0.98*	*0.96*
Nozzle diameter (mm)	*0.2*	*0.2*	*0.2*
Fiber diameter(µm)	*35±13*	*11±6*	*4±2*

2.3 Composite assembling

In order to produce hybrid assemblies, only sample B (fibers with 11 µm diameter) mats were considered for characterization purpose. However, regarding the valve fatigue testing procedure, both sample A and sample B mats obtained respectively from fine and coarse fibers were used in order to study the influence of the fiber diameter on the durability of the hybrid textile valve.

For all materials the non-woven mat obtained with the force spinning system was deposited on the surface of a woven PET substrate plain weave (75 yarns/cm in warp, 50 yarns/cm in weft, density 73.7 g/m^2, yarn count 50 dtex, multifilament).

In order to create an adherence between the 2 layers, different assembly methods were investigated (Figure 3):

- Sewing the two layers together using a 22 dtex multifilament PET yarn according to the sewing pattern presented in Figure 3 A.
- Creating local melted areas using an ultrasonic welding gun (ultrasonic fusion is applied according to the pattern presented in Figure 3 B).
- Using a biomedical grade adhesive (Cryolife BioGlue surgical adhesive). Pattern presented in Figure 3 C shows the adhesive matrix.

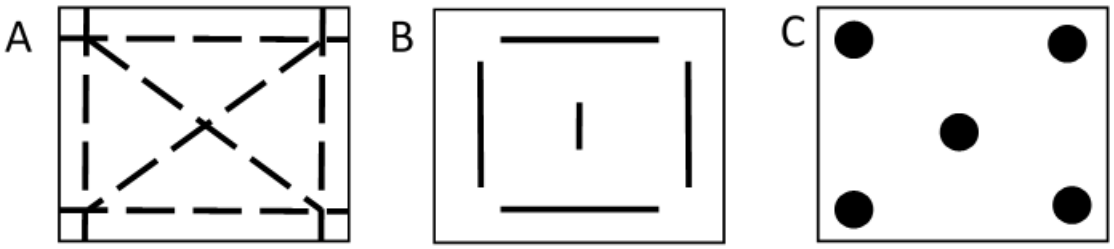

Figure 3. Patterns used in (A) sewing assembly (B) ultrasonic assembly (C) biomedical adhesive assembly.

2.4 Material characterization

Characterization tests have been performed in order to assess the influence of the added layer and the assembling process on some physical parameters, which are critical for the heart valve and the material performances (thickness, roughness, permeability, bending stiffness, pore size) using standard testing equipment.

2.4.1 Thickness

Leaflet thickness was measured with a dedicated instrument (C110T, Kroeplin GmbH, Schlüchtern, Germany). The applied force during the measurement was 0.5 gf/cm², which corresponds to the sensitivity of the device used.

2.4.2 Surface roughness

Surface roughness was assessed in order to investigate the surface topography modifications induced by the assembling. Roughness given as a standard mean deviation (SMD) value in µm was measured with a Kawabata's Evaluation System instrument (KES-FB4, KATO TECH Co., LTD., Kyoto, Japan).

2.4.3 Permeability

In order to assess the permeability of each fabric (ISO 7198), square textile specimens (1 cm^2) were placed under a static water column applying a 120-mmHg pressure over the specimen. Flow across the fabric was measured (L/min) over a 3-min period of time.

2.4.4 Bending stiffness

The bending stiffness of the fabric was measured with the cantilever method (ISO 9073-7, Shirley Stiffness Tester). The goal was to ensure that the added non-woven layer keeps the leaflet enough flexible.

2.4.5 Surface density and pore size

In order to assess geometrical characteristics of the non-woven mats surface, images of the sample surfaces were recorded with an optical microscope (x8) (VHX 6000, Keyence, Courbevoie, France). The resulting images were then processed to be converted in black and white and the surface pore density was defined as the ratio of black pixels to the overall area. Moreover, as pore size and pore density are not necessarily correlated, the pore size was measured by segmenting the images into squares (28 pixels x 36 pixels). The calculation of the ratio of black pixels to the area of each square was further considered as the pore area. Despite the fact that the method provides only average values it enables to compare the different non-woven textile structures to each other.

2.4.6 Thermal crystallinity

Given that the degree of crystallinity is an important feature that affects the mechanical properties of the non-woven mat, differential Scanning Calorimetry (DSC) was performed on the non-woven samples using a Mettler TOLEDO DSC 823^e instrument to determine their crystallinity. DSC thermographs were obtained according to the following procedure: the samples were held during 2min at 25°C then heated from 25°C to 300°C at 5°C/min (first heating cycle) then cooled to 25°C at -20°C/min and held at 25°C during 2 minutes (cooling cycle) and finally reheated to 300°C at 5°C/min (second heating cycle) under a nitrogen atmosphere. The crystallinity was determined using the equation:

$$X_c = \left[\frac{\Delta H_m - \Delta H_{cc}}{\Delta H_c}\right] \times 100 \quad (2)$$

Where ΔH_m is heat of melting, ΔH_{cc} is the heat of cold crystallization and ΔH_c is the heat of melting for 100 % crystalline PET.

2.5 Valve manufacturing

After having characterized the performances of the obtained hybrid material, valve specimens were manufactured according to a procedure already described in a previous work[22] and based on

a thermal shape fixation treatment. However, the non-woven layer being easily damaged with thermal treatment, the usual procedure was modified in order to prevent the non-woven material from being heated. For that purpose, the valve was first shaped from a woven PET substrate without the non-woven layer, which was added separately in a second time according to following steps:

- The PET woven textile flat membrane initially sewn in a tubular geometry was shaped in a valve form under heating conditions (110°C, 40 min). The design of the valve was obtained from the geometry of the mold used to shape the cusps. The mold is characterized by 3 cylindrical shapes (same radius as the valve radius), which are prolonged with triangular surfaces for leaflet coaptation purpose (Figure 4 A, B and C).
- The shaped fabric woven tube was then opened along the length and assembled in a 2D configuration with the non-woven layer using the previously described assembling methods (Figure 4 D). Over the assembling, the non-woven mat follows the shape given to the woven fabric cusps.
- The hybrid fibrous construct was welded along the height in order to obtain a hybrid shaped tube. The shaped valves were then assembled with commercially available 23 mm biological valve rings from which the biological tissue had been removed. Ethicon monofilament suture yarn Prolene 5-0 was used (Figure 4 E and F).

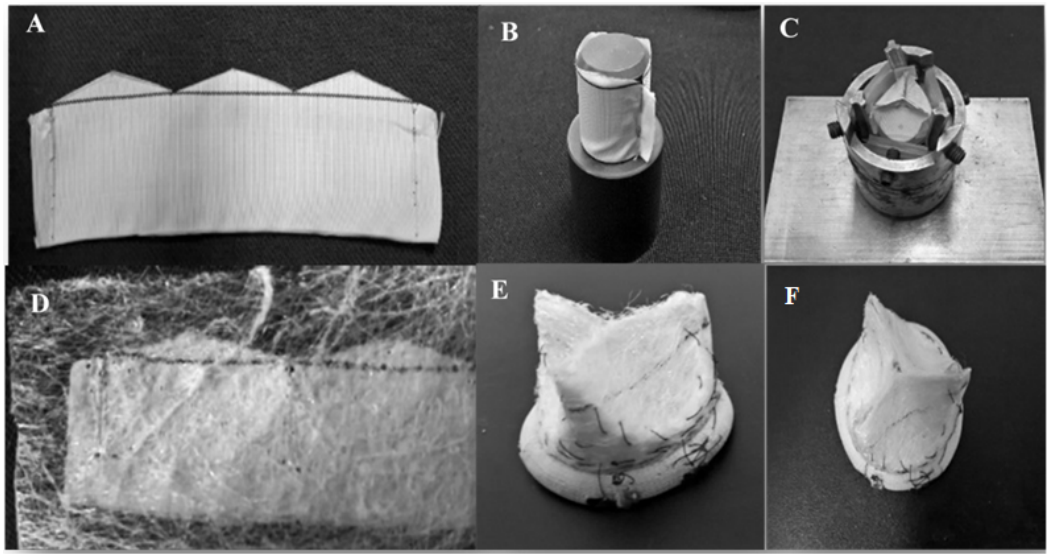

Figure 4. (A) Trileaflet design (B) Tubular shape (C) Valve shaping (D) Valve assembling (E) Hybrid valve (side view) (F) Hybrid valve (top view).

2.6 Valve performances

The durability of the hybrid heart valves (obtained from sample A and sample B non-woven materials) was assessed using an accelerated fatigue tester (ViVitro Labs HiCycle System) according to the ISO 5840 standard. The pressure applied on the valve was set to 100 ± 5 mmHg and the valves were cycled at 14 Hz. At regular time intervals, the valve specimens were observed macroscopically in order to identify material degradations and assess the durability of the various assembling processes.

3 RESULTS AND DISCUSSION

3.1 Non-woven mat properties

Table 2 presents detailed features of the 2 mats, which were considered in the frame of this study (sample A and sample B). While fiber size was different in the 2 materials, surface density values

as well as average pore size values remained similar. This allowed to investigate the influence of the sole fiber size on the global mat behavior.

Table 2. Non-woven characteristics.

	Sample A	Sample B
Average fiber diameter (µm)	35 ±13	11±6
Surface density (%)	57±2	61±4
Average pore size (µm)	47±1	45±3
3D porosity (%)	82.29	81.12
Crystallinity (%)	10.52	27.65

One can observe that the crystallinity rate increases when the fiber size goes down. This will have an influence on the mechanical strength of the valve leaflets and the durability of the valves, which will be discussed later.

3.2 Material characterization

Results presented in figure 5 bring out that the non-woven layer increases the bending stiffness and the roughness of the material in a significant way, whatever the assembling process, which is considered. Conversely the permeability is only slightly reduced. However, some differences could be observed between the various assembling techniques.

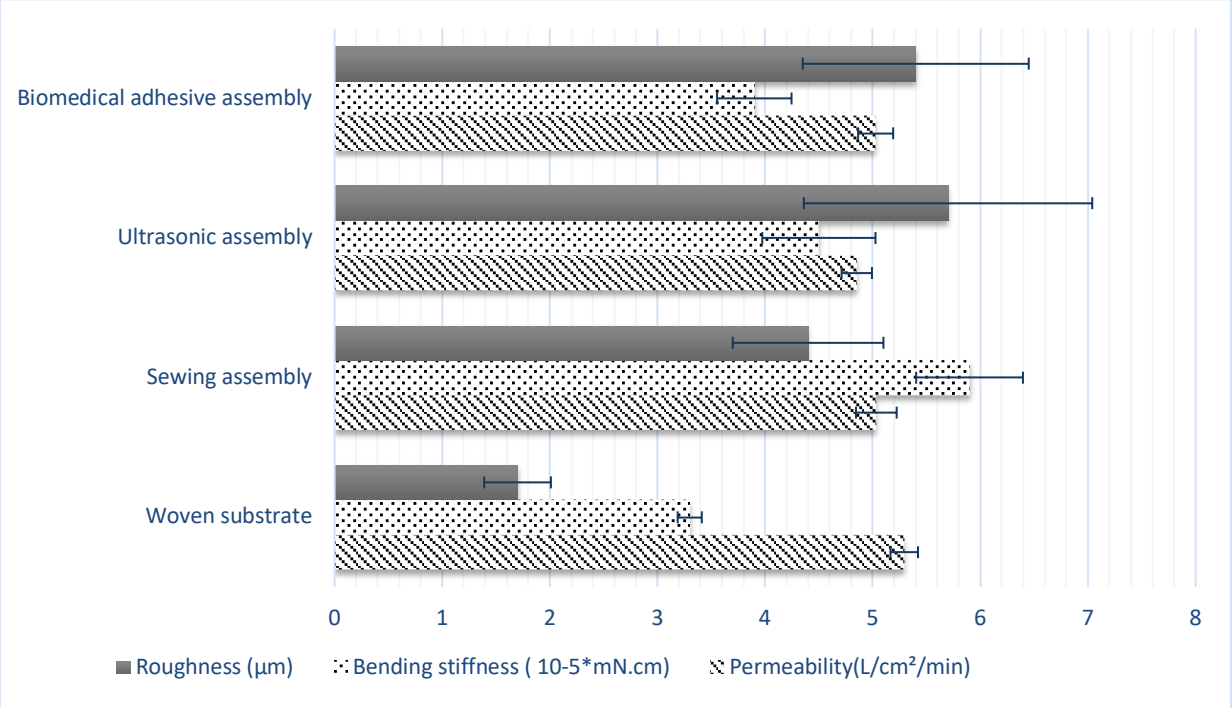

Figure 5 Characteristics of the composite fibrous construct according to the different assembling techniques

3.2.1 Thickness

As expected, the added non-woven layer resulted in increasing the thickness, which raised respectively from 120 to 342, 430 and 447 µm for the ultrasonic, sewing and biomedical adhesive assembly. The thermal treatment applied locally to the ultrasonic assembly resulted in local

thickness reduction compared to the other assembly techniques. These values remain below values that characterize bovine pericardium in clinical use.

3.2.2 Roughness

Regarding the roughness, results bring out that all the assembling techniques tend to modify the topography of the surfaces. The roughness value is increased by nearly a factor 3 regardless of the considered process. It is however notable that in the sewn material the roughness generated by the stitch points is slightly limited compared to the bonds obtained with the other techniques (44, 54 and 57 µm for respectively the sewing assembly, biomedical adhesive assembly and ultrasonic assembly). The roughness is thus slightly reduced.

3.2.3 Permeability

It can be observed in figure 5 that by adding a non-woven layer on the woven substrate, the permeability is only slightly reduced by around 5% for all processes. Actually, the pores in the woven material are slightly obstructed with the non-woven fibers, but with no significant difference between the various samples.

3.2.4 Stiffness

It could be observed that the added non-woven layer generates globally a stiffness increase whatever the assembling process which is considered (by 18% for the biomedical adhesive assembly and 78% for the sewing assembly). Actually, the 3 techniques generate a discontinuous assembling pattern, characterized by assembling points regularly spread over the surface of the textile. These points tend to rigidify the material locally. The fibers cannot slide over each other anymore in the vicinity of these points when the textile is flexed, limiting the flexure amplitude. However, fibers still have the opportunity to move and slide over each other between 2 neighbor fixation points. The fibrous construction keeps thus globally some flexibility.

When comparing the assembling techniques in more detail, one can observe in particular that the stiffness increase is more critical with the sewing process compared to the 2 other techniques (5.9×10^{-5}, 4.5×10^{-5} and 3.9×10^{-5} mN.cm for respectively the sewing assembly, ultrasonic assembly and biomedical adhesive assembly). Actually, the sewing tends to tighten the fibers together along the whole sewing line while the other techniques just create local fixation points. Nevertheless, one can assume that once the material is flexed in a cyclic way, the discontinuity induced by the suture yarn will allow fibrous rearrangement in the construction as was described in previous work[23]. Heim et al. cycled textile strips of various construction under flexure conditions and brought out that yarns and fabric tend to adapt to the load applied towards a configuration with limited stress. The stiffness generated at assembling level should decrease with time over the cycling process.

Tests performed in a heart pulse duplicator with valves obtained from the various hybrid textiles showed that the stiffness increase described above didn't modify the closing time and the regurgitation of the valve.

3.3 Valve manufacturing

Valves were obtained from both non-woven mats presented in the previous section. Their characteristics are presented in Table 3

Table 3 Valves characteristics

	Valve 1 (sample A)	Valve 2 (sample B)
Thickness(µm)	430±19	334±1
Roughness ;SMD (µm)	7±1	5±1
3D porosity (%)	74.75	71.80

3.3.1 Fatigue testing

The fatigue tests brought out various results depending on: (1) the assembling technique, which was considered, (2) the non-woven characteristics.

3.3.1.1 Influence of the assembling process

When comparing the different assembling techniques, only the sample A mat was considered. Results bring out that the performances of the biomedical adhesive and the ultrasonic assembly presented similarities. Various degradation phenomena could be observed.

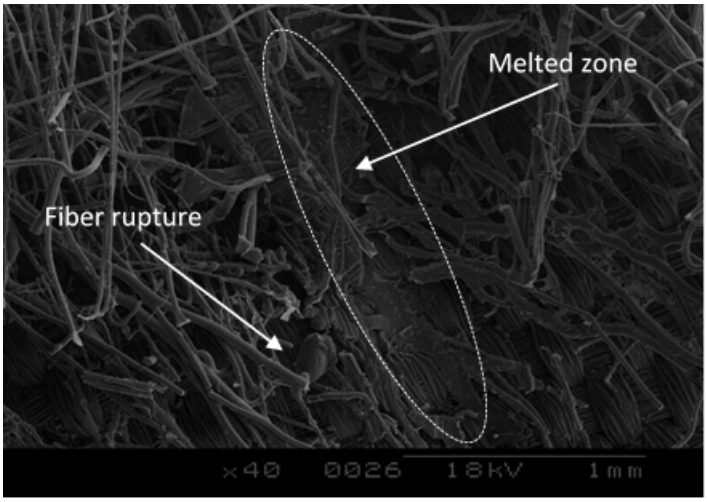

Figure 6. SEM image at an ultrasonic locally melted zone after cycling

First, in both cases, the fixation points underwent fracture under the cyclic loading due to the local rigidity induced in the material either by the adhesive bond or the ultra-sonic locally melted zone. Second, the fibers embedded in the rigid fixation point matrix tended to brake after cycling (Figure 6). Actually, the fibers are blocked on one side in the either melted or sticked zone while the other end undergoes cycling flexure. This flexure tends to induce crack propagation related to fatigue stress. Actually, a fiber embedded in the fixation point matrix can be approximated as a beam, which is fixed at one end. According to the strength of material theory, the stress on the fixed side is the highest, which leads to material rupture over time. The phenomenon is particularly visible for the adhesive assembling for which cracks propagated already after only a limited number of cycles (0.2 Mio) over the whole surface of the fabric. Globally, the adhesive technique was definitely not compatible with the heart valve requirements. This material was thus not tested further.

Regarding the ultrasonic assembly, damages were observed in more localized areas due to the fact that the size of the bonds could be smaller with that technique, providing more movement freedom to the fibers, and thus limiting the degradation phenomenon.

Finally, the sewing assembly appeared to be the most durable assembling method as the first degradations were observed only after 10 Mio cycles. While only limited fiber breakages could be observed and while the sewing yarn remained undamaged, a loss of cohesion in the non-woven mat could, however, be identified along the suture lines over the cycling process. Regarding that latter issue, the cohesion of 2 non-woven mats produced with different characteristics were compared and analyzed more precisely in a second step in order to better understand the degradation phenomenon.

3.3.1.2 Influence of the mat characteristics on the cohesion of the hybrid material

When comparing the durability of hybrid fabrics made from sample A and sample B, it was observed that a loss of cohesion occurred in valve 1 (large fibers) after 10 Mio and in valve 2 (small fibers) after only 4 Mio. SEM images of both structures after cycling show similar degradation patterns occurring, however, at different time points. A closer look to the degraded material brings out that 2 main degradation mechanisms can be identified: (1) fiber rupture; (2) delamination at free edge level.

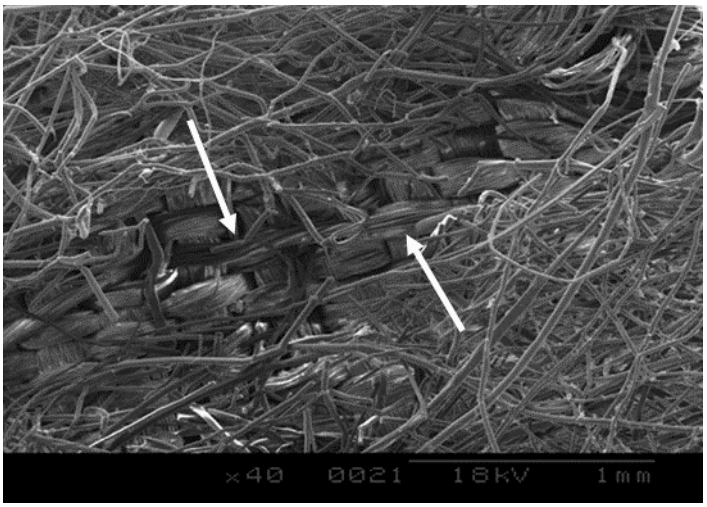

Figure 7. SEM image of the degradation undergone by the fibers after cycling.

Regarding fiber breakage, a closer look at the rupture facies (fiber cross section) shows that the fibers underwent rupture at suture lines level due to axial loading (Figure 7). Basically, the non-woven material located between neighbor suture lines is highly solicited by the water cyclic flow. The flow tends to move the non-woven material around locally. Consequently, tension is generated within the fibers squeezed under the suture line. They deform plastically, and eventually brake. This occurs in particular when the bonds between neighbor fibers in the mat are not strong enough to spread the load equally over the whole surface.

Moreover, it could be observed that the breakage occurred later in valve 1 made from larger fibers despite the materials are produced with similar density and pore size (around 60%). This may be due to the difference in stiffness, which is one of the most fundamental properties for a fiber. At molecular scale, with higher crystallinity rate the degree of freedom of molecular chains is limited in a material, which makes it stiffer. In our case, DSC results show that sample B material is characterized by a higher crystallinity rate, which is almost 3 times as high as for sample A (from 10.52 to 27.65).

These results are in correlation with what have been demonstrated in the literature. Kwon et al prepared PCLPL meshes with fiber diameter of 0.2, 1.7 and 7 microns and found out that the smaller fiber meshes were stiffer than the larger (Young's moduli of 2.2, 1.8, 0.8 MPa respectively) (Kwon et al 2005). These results can be explained with the polymer morphology. Wong et al used X ray diffraction and single fiber tensile testing and demonstrated that stiffer smaller diameter PCL fiber exhibit higher degrees of crystallinity and molecular orientation compared to softer large diameter fibers (Wong et al 2008). Actually, fibers with small diameters are spun at high temperature (in order to reduce the polymer viscosity), which tends to limit their elasticity and make them more fragile. Globally, whatever the non-woven characteristics, one can expect that this degradation will be very limited in vivo. Minimal tissue ingrowth will occur and stabilize the whole structure.

With respect to the delamination between the non-woven layer and the woven substrate, it occurred at the level of the free edge. In this zone the 2 layers were assembled along a melted line created with an ultrasonic gun. Fibers are thus embedded in a local melted polymer matrix and tend to get broken as already described in the previous section due to local high flexure stress.

3.3.1.3 Hybrid textile production strategies

The force spinning system used in this study allowed obtaining non-woven PET mats at the laboratory scale for the purpose of concept validation. In order to make the production of fibers more reliable at a larger scale, other non-woven fiber production technologies could be considered in future work. First, the non-woven melt blowing process can be used for the production of fibers in the micrometer and smaller scale from melted polymer. The process, in which the polymer drawing is performed by an air jet, is very versatile and already largely used to produce filtering fibrous mats. In this industrial field the typical average fiber size is below 30 µm[26]. But it has been shown that smaller fiber sizes in the micro and even nano diameter range can also be obtained with the process, when the production parameters like viscosity or temperature are precisely adjusted[27, 28].

Melt electrospinning is another process suited for the non-woven mat production. This technology becomes more and more popular and has been already largely used for tissue engineering applications[29]. The process principle is based on electrostatic fiber drawing of melted polymer. It presents the advantage of increasing the fiber output vs. solvent electrospinning and alleviates the issues related to the use of solvents. In the beginning, the process was not very competitive with melt blowing as fiber production was in the tens of micron diameter range, while the process was more complicated to set up. But recent advances have shown that the process parameters can be set in order to obtain fibers of smaller size[30].

Finally, any of these more industrial non-woven pro- duction techniques could be used in future work to better control the non-woven mat tight specifications, which are required for hybrid textile applications. Moreover, these mats could be advantageously directly sprayed on the woven substrate before being sewn, as these processes provide a unidirectional fiber output compared to force spinning.

4 CONCLUSIONS

In this study the physical characteristics and mechanical performances of a novel hybrid fibrous construction for heart valve application were studied. By tuning the adjustment parameters of a force spinning process it was possible to produce non-woven PET mats characterized by small fiber diameter and large pore size. Various assembling techniques were considered to assemble the mats with a woven substrate. The added layer increased slightly the stiffness and the roughness properties of the substrate in all cases while the permeability remained stable. Despite these modifications, the dynamic behavior of valves made from any of the hybrid textile tested didn't change over one cardiac cycle in vitro. Regarding the long-term behavior under accelerated cyclic

loading conditions, sewing seems to present an advantage as the sewn hybrid material is the most durable. However, degradations could be observed in the non-woven mat after 4 Mio cycles along the suture line especially when small fibers are considered. If one can assume that slight tissue in-growth is expected to stabilize the structure in vivo, the small fibers production should be better controlled in future work in order to increase the strength of the obtained fibers.

ACKNOWLEDGEMENTS

Author Statement
Research funding: Authors state no funding involved.
Conflict of interest: Authors state no conflict of interest. Informed consent: Informed consent is not applicable. Ethical approval: The conducted research is not related to either human or animals use.

REFERENCES

1. McCabe, J.M. et al, 2016. Surgical Versus Percutaneous Femoral Access for Delivery of Large-Bore Cardiovascular Devices (from the PARTNER Trial). The American Journal of Cardiology 117, 1643–1650. doi:10.1016/j.amjcard.2016.02.041
2. Cribier, A., 2002. Percutaneous Transcatheter Implantation of an Aortic Valve Prosthesis for Calcific Aortic Stenosis: First Human Case Description. Circulation 106, 3006–3008. doi:10.1161/01.CIR.0000047200.36165.B8
3. Yoon, S.-H et al ,2017. Outcomes in Transcatheter Aortic Valve Replacement for Bicuspid Versus Tricuspid Aortic Valve Stenosis. Journal of the American College of Cardiology 69, 2579–2589. doi:10.1016/j.jacc.2017.03.017
4. Dijkman, P.E., Fioretta, E.S., Frese, L., Pasqualini, F.S., Hoerstrup, S.P., 2016. Heart Valve Replacements with Regenerative Capacity. Transfusion Medicine and Hemotherapy 43, 282–290. doi:10.1159/000448181
5. Zegdi, R., Ciobotaru, V., Noghin, M., Sleilaty, G., Lafont, A., Latrémouille, C., Deloche, A., Fabiani, J.-N., 2008. Is It Reasonable to Treat All Calcified Stenotic Aortic Valves With a Valved Stent? Journal of the American College of Cardiology 51, 579–584. doi:10.1016/j.jacc.2007.10.023
6. Kiefer, P. et al. Crimping may affect the durability of transcatheter valves: an experimental analysis. The Annals of Thoracic Surgery 2011; 92(1), 155-160. doi:10.1016/j.athoracsur.2011.03.020
7. Alavi, S.H., Groves, E.M., Kheradvar, A., 2014. The Effects of Transcatheter Valve Crimping on Pericardial Leaflets. The Annals of Thoracic Surgery 97 ,1260–1266. doi:10.1016/j.athoracsur.2013.11.009
8. Dvir, D. Half of transcatheter heart valves show degeneration within 10 years of TAVI. EuroPCR 2016. Session: tuesday 17 May 11.20-12.20, Late-breaking trials, registries and innovations
9. Vaesken, A., Heim, F., Chakfe, N., 2014. Fiber heart valve prosthesis: Influence of the fabric construction parameters on the valve fatigue performances. Journal of the mechanical behavior of biomedical materials 40, 69-74. doi:10.1016/j.jmbbm.2014.08.015
10. Cao, H. et al, 2010. The topographical effect of electrospun nanofibrous scaffolds on the in vivo and in vitro foreign body reaction.Journal of Biomedical Materials Research 93A ,1151-1159.
11. Bellon, J. M. et al ,1998.Tissue response to polypropylene meshes used in the repair of abdominal wall defects.Biomaterials, 19, 669-675. doi :10.1016/S0142-9612(97)00162-2
12. Klosterhalfen, B., Klinge, U., Schumpelick, V., 1998.Functional and morphological evaluation of different polypropylene-mesh modifications for abdominal wall repair. Biomaterials 19, 2235-2246.
13. Klosterhalfen, B.,Junge K., Klinge, U.,2005.The lightweight and large porous mesh concept for hernia repair.Expert Review of Medical Devices, 2, 103-117. doi :10.1586/17434440.2.1.103

14. Vaesken, A. , Pelle, A., Pavon-Djavid, G., Rancic, J., Chakfe, N., Heim, F.,2017.Heart valves from polyester fibers: a preliminary 6-month in vivo study.Biomedical Engineering / Biomedizinische Technik. doi:10.1515/bmt-2016-0242
15. Tian, F., Hosseinkhani, H., Hosseinkhani, M., Khademhosseini, A., Yokoyama, Y., Estrada, G.G., Kobayashi, H., 2008. Quantitative analysis of cell adhesion on aligned micro- and nanofibers. Journal of Biomedical Materials Research, 84A, 291–299. doi:10.1002/jbm.a.31304
16. Lowery, J.L., Datta, N., Rutledge, G.C., 2010. Effect of fiber diameter, pore size and seeding method on growth of human dermal fibroblasts in electrospun poly(ε-caprolactone) fibrous mats. Biomaterials 31, 491–504. doi:10.1016/j.biomaterials.2009.09.072
17. Sanders, J.E., Cassisi, D.V., Neumann, T., Golledge, S.L., Zachariah, S.G., Ratner, B.D., Bale, S.D., 2003. Relative influence of polymer fiber diameter and surface charge on fibrous capsule thickness and vessel density for single-fiber implants. Journal of Biomedical Materials Research Part A 65, 462–467.
18. Hodgkinson, T., Yuan, X.-F., Bayat, A., 2014. Electrospun silk fibroin fiber diameter influences in vitro dermal fibroblast behavior and promotes healing of ex vivo wound models. Journal of tissue engineering 5, 2041731414551661.
19. Haller, N. et al, 2013. Noninvasive analysis of synthetic and decellularized scaffolds for heart valve tissue engineering. ASAIO 59(2),169-77. DOI: 10.1097/MAT.0b013e31827db6b6
20. Kucinska-Lipka, J., Gubanska, I., Janik, H., Sienkiewicz, M., 2015. Fabrication of polyurethane and polyurethane based composite fibres by the electrospinning technique for soft tissue engineering of cardiovascular system. Material Science and Engineering C46,166–176. doi :10.1016/j.msec.2014.10.027
21. Amoroso, N.J., D'Amore, A., Hong, Y., Rivera, C.P., Sacks, M.S., Wagner, W.R., 2012. Microstructural manipulation of electrospun scaffolds for specific bending stiffness for heart valve tissue engineering. Acta Biomaterialia 8, 4268–4277. doi:10.1016/j.actbio.2012.08.002
22. Heim, F., Durand, B., Chakfe, N., 2008.Textile heart valve prosthesis: Manufacturing process and prototype performances. Textile Reseach Journal 78 ,1124-1131.
23. Heim F, Gupta B. Textile Heart Valve Prosthesis: The effect of Fabric Construction Parameters on Long Term Durability. Text Res J 2009; 79: 1001-1013.
24. Kwon IK, Kidoaki S, Matsuda T. Electrospun nano- to microfiber fabrics made of biodegradable copolyesters: structural char- acteristics, mechanical properties and cell adhesion potential. Biomaterials 2005;26:3929–39.
25. Wong SC, Baji A, Leng S. Effect of fiber diameter on tensile properties of electrospun poly(ε-caprolactone). Polymer 2008;49:4713–22.
26. Bhat G, Malkan S. Polymer-laid web formation. In: Russel SJ, editor. Handbook of nonwovens. Cambridge: Woodhead Publishing Ltd. 2007:143–200.
27. Dutton KC. Overview and analysis of the meltblown process and parameters. J Text Apparel Technol Manage 2008;6:1–24.
28. Nayak R, Padhye R, Arnold L, Kyratzis IL, Truong YB, Peeters G, et al. Mechanism of nanofibre fabrication by meltblowing. Appl Mech Mater 2012;217:207–12.
29. Ristovski N, Bock N, Liao S, Powell SK, Ren J, Kirby GT, et al. Improved fabrication of melt electrospun tissue engineering scaffolds using direct writing and advanced electric field con- trol. Biointerphases 2015;10:011006.
29. Brown T, Dalton P, Hutmacher D. Melt electrospinning today: an opportune time for an emerging polymer process. Prog Polym Sci 2016;56:116–66.